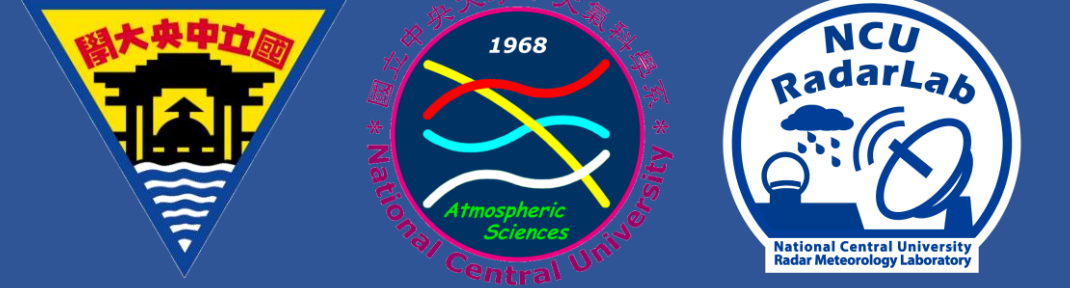


A new method to determine the unknown constants on each horizontal layer in thermodynamic retrieval using multiple-Doppler-radar synthesized winds

Yu-Chiang Liou and Yung-Lin Teng

Department of Atmospheric Sciences, National Central University, Zhongli, Taoyuan City, Taiwan



ABSTRACT

One can apply thermodynamic retrieval (TR) technique to retrieve pressure and temperature perturbations in a 3D space using wind fields synthesized by Doppler radars. However, a long-lasting problem is that an unknown constant exists on each horizontal level, leading to the ambiguity in the retrieved vertical structure of the thermodynamic variables. In this research the widely-used TR scheme first proposed in 1978 is improved by implementing **the Equation of State** so that the unknown constant at each layer can be explicitly identified and removed from the retrieved 3D thermodynamic fields. The only in-situ independent observations needed for the correction is the pressure and temperature measured at a single station, which can be located at surface, mountain slope, or on board an airborne Doppler radar.

1. The unknown constant problem in the widely-used TR method (Gal-Chen 1978, hereafter G78)

The G78 thermodynamic retrieval starts with the momentum equations:

$$-F \equiv \frac{1}{\theta_{v0}} \left[\frac{\partial u}{\partial t} + \vec{V} \cdot \nabla u - f v + \text{turb}(u) \right] = -\frac{\partial \pi'}{\partial x} \quad (1)$$

$$-G \equiv \frac{1}{\theta_{v0}} \left[\frac{\partial v}{\partial t} + \vec{V} \cdot \nabla v + f u + \text{turb}(v) \right] = -\frac{\partial \pi'}{\partial y} \quad (2)$$

$$-H \equiv \frac{1}{\theta_{v0}} \left[\frac{\partial w}{\partial t} + \vec{V} \cdot \nabla w + \text{turb}(w) + g(q_r + q_s) \right] = -\frac{\partial \pi'}{\partial z} + g \frac{\theta'_c}{\theta_{v0} \theta_0} \quad (3)$$

The F , G , and H can be obtained once the 3D air motion is obtained through multiple-Doppler-radar synthesis (e.g. Liou et al. 2012).

In G78 a cost function J_I is formulated over a given horizontal plane using (1) and (2):

$$J_I = \iint \left[\left(\frac{\partial \pi'}{\partial x} - F \right)^2 + \left(\frac{\partial \pi'}{\partial y} - G \right)^2 \right] dx dy \quad (4)$$

A set of π' which minimizes J_I can be found by solving a Poisson equation for π'

$$\frac{\partial^2 \pi'}{\partial x^2} + \frac{\partial^2 \pi'}{\partial y^2} = \frac{\partial F}{\partial x} + \frac{\partial G}{\partial y} \quad (5)$$

subject to the Neumann boundary conditions

$$\frac{\partial \pi'}{\partial x} = F, \text{ at } x = x_w, x_e \quad (6a)$$

$$\frac{\partial \pi'}{\partial y} = G, \text{ at } y = y_s, y_n \quad (6b)$$

Due to the use of (6a) and (6b), the solutions of (5) can be satisfied only up to an arbitrary constant. G78 proposed that the unique solution from (5) is $\pi' - \langle \pi' \rangle$, where $\langle \rangle$ represents a horizontal average. After rewriting (3), making a horizontal average and computing the difference, we have:

$$\frac{\partial(\pi' - \langle \pi' \rangle)}{\partial z} = g \frac{\theta'_c - \langle \theta'_c \rangle}{\theta_{v0} \theta_0} + (H - \langle H \rangle) \quad (7)$$

Substituting the retrieved $\pi' - \langle \pi' \rangle$ into (7), one can solve for $\theta'_c - \langle \theta'_c \rangle$.

To get $\langle \pi' \rangle$ on a given horizontal layer, a single-point of in-situ observation of π' on this layer combined with the G78-retrieved $\pi' - \langle \pi' \rangle$ at this point is sufficient to determine the $\langle \pi' \rangle$ of this layer, from which π' itself can be computed at all points over the entire layer. This procedure is repeated for each layer and for $\langle \theta'_c \rangle$. Regarding the single-point in-situ observations on each layer, previous studies proposed aircraft or radiosonde/dropsonde. However, an aircraft is not available in routine operations, and the temporal resolution of radiosonde/dropsonde is too low.

2. The Equation of State (EoS)

The equation of state (EoS) links the absolute pressure with the temperature fields, thus is implemented and written as follows. Detailed derivation can be found in Liou and Teng (2023).

$$\theta'_c = \tilde{T}_1 \pi' - \tilde{T}_2 \rho' \quad (8)$$

$$\tilde{T}_1 = \left[\left(\frac{P_{00}}{P_0} \right)^\kappa \frac{1}{\rho_0 R (1 + 0.61 q_{v0})} - \frac{R}{C_p} \frac{\theta_0}{P_0} \right] \frac{P_0}{R} \left(\frac{P_{00}}{P_0} \right)^\kappa \quad (9a)$$

$$\tilde{T}_2 = \left(\frac{P_{00}}{P_0} \right)^\kappa \frac{T_0}{\rho_0} \quad (9b)$$

3. The new thermodynamic retrieval approach

The EoS in (8) introduces an additional unknown variable ρ' , therefore it is desirable to find places where the influence from ρ' on (8) is minimal. Using the data generated by the numerical simulation of a thunderstorm, it is found that $|\rho'|$ is highly correlated with $|\theta'_c|$. As a result, $|\theta'_c|$ can be used as an index to find small $|\rho'|$.

A procedure for determining the unknown $\langle \pi' \rangle$ and $\langle \theta'_c \rangle$ profiles is explained in the following:

Step (1): Assuming F , G , and H are available in (1)-(3), use G78 method to retrieve $\pi' - \langle \pi' \rangle$ and $\theta'_c - \langle \theta'_c \rangle$ at each grid point in the 3D space.

Step (2): A set of π' and θ'_c on the first layer measured at a station is combined with the G78-retrieved $\pi' - \langle \pi' \rangle$ and $\theta'_c - \langle \theta'_c \rangle$ to get $\langle \pi' \rangle$ and $\langle \theta'_c \rangle$ of the first layer. Applying this set of $\langle \pi' \rangle$ and $\langle \theta'_c \rangle$ to other points to get the π' and θ'_c at all points on the first layer.

Step (3): Find those surface grid points where the $|\theta'_c|$ s are the smallest 10% of all grids on the first layer. Suppose one of such grid point A is located at $(X_A, Y_A, 1)$, one can use its θ'_c and H to integrate (3) upward starting from the π' at $(X_A, Y_A, 1)$ to obtain the π' on the second layer at $(X_A, Y_A, 2)$. By combining this π' with the G78-retrieved $\pi' - \langle \pi' \rangle$ at this grid point yields the $\langle \pi' \rangle$ of the second layer.

Step (4): Using π' on the second layer at point $(X_A, Y_A, 2)$ and the EoS in (8) to estimate θ'_c at the same point. By combining this with the G78 retrieved $\theta'_c - \langle \theta'_c \rangle$ at this point yields the $\langle \theta'_c \rangle$ of the second layer. When applying (8), ρ' is taken from the grid one layer below.

Step (5): Step (3) and Step (4) are repeated from the second layer until $Z=1.0$ km.

Step (6): For each surface grid point whose $|\theta'_c|$ is the smallest 10% of all grids, Steps (2)-(5) are performed to obtain a set of $\langle \pi' \rangle$ and $\langle \theta'_c \rangle$ profiles. An average is made over the multiple profiles produced by the vertical integration starting from each of those selected points.

Step (7): From $Z=1.0$ km, Steps (2)-(6) resume until the stepwise upward integrations reach domain top.

4. Results from OSSE tests

Figure 1 shows in the OSSE tests the retrieved $\langle \pi' \rangle$ and $\langle \theta'_c \rangle$ profiles agree with their true counterparts very well. Figure 2 depicts the true and retrieved thermodynamic fields over a vertical cross section. The vertical structure of the thermodynamic fields (π' and θ'_c), instead of their deviations from horizontal averages, are correctly resolved. The RMSE are reduced from 0.24 J kg⁻¹ K⁻¹ to 0.01 J kg⁻¹ K⁻¹ for π' , and from 0.73 K to 0.22 K for θ'_c , respectively. The Spatial Correlation Coefficient (SCC) can be improved from approximately 0.65 to at least 0.97 for both thermodynamic variables.

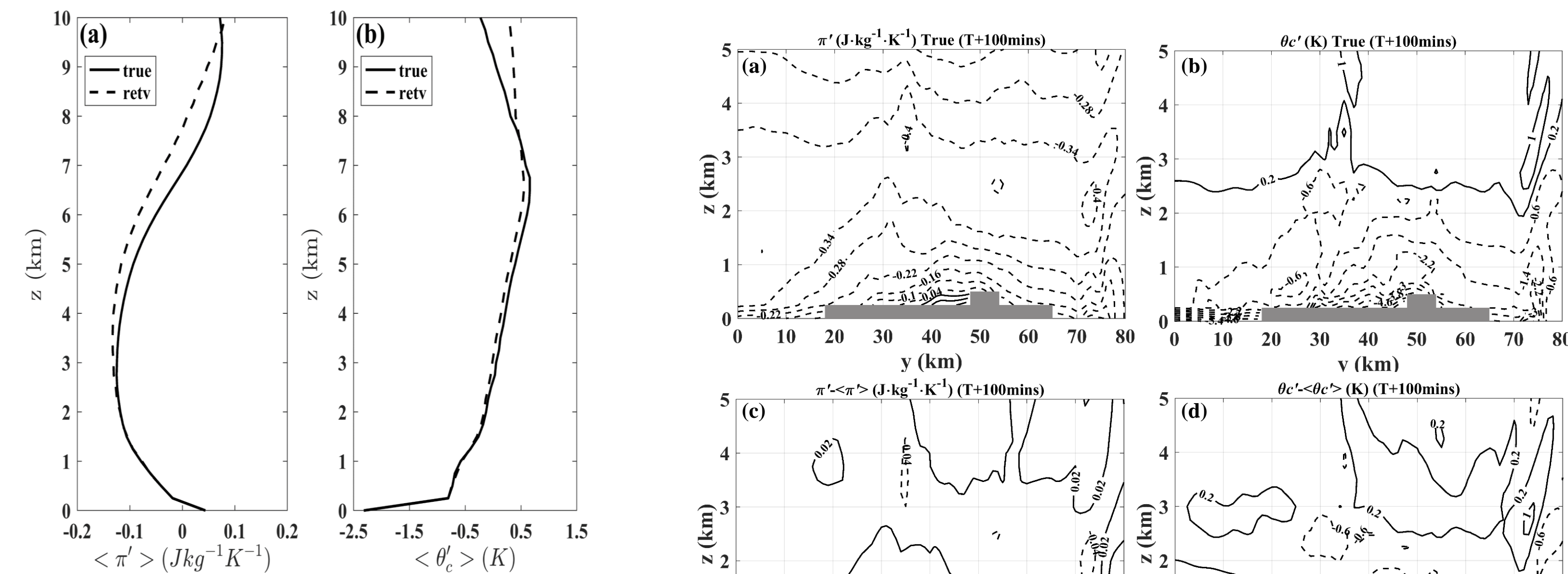
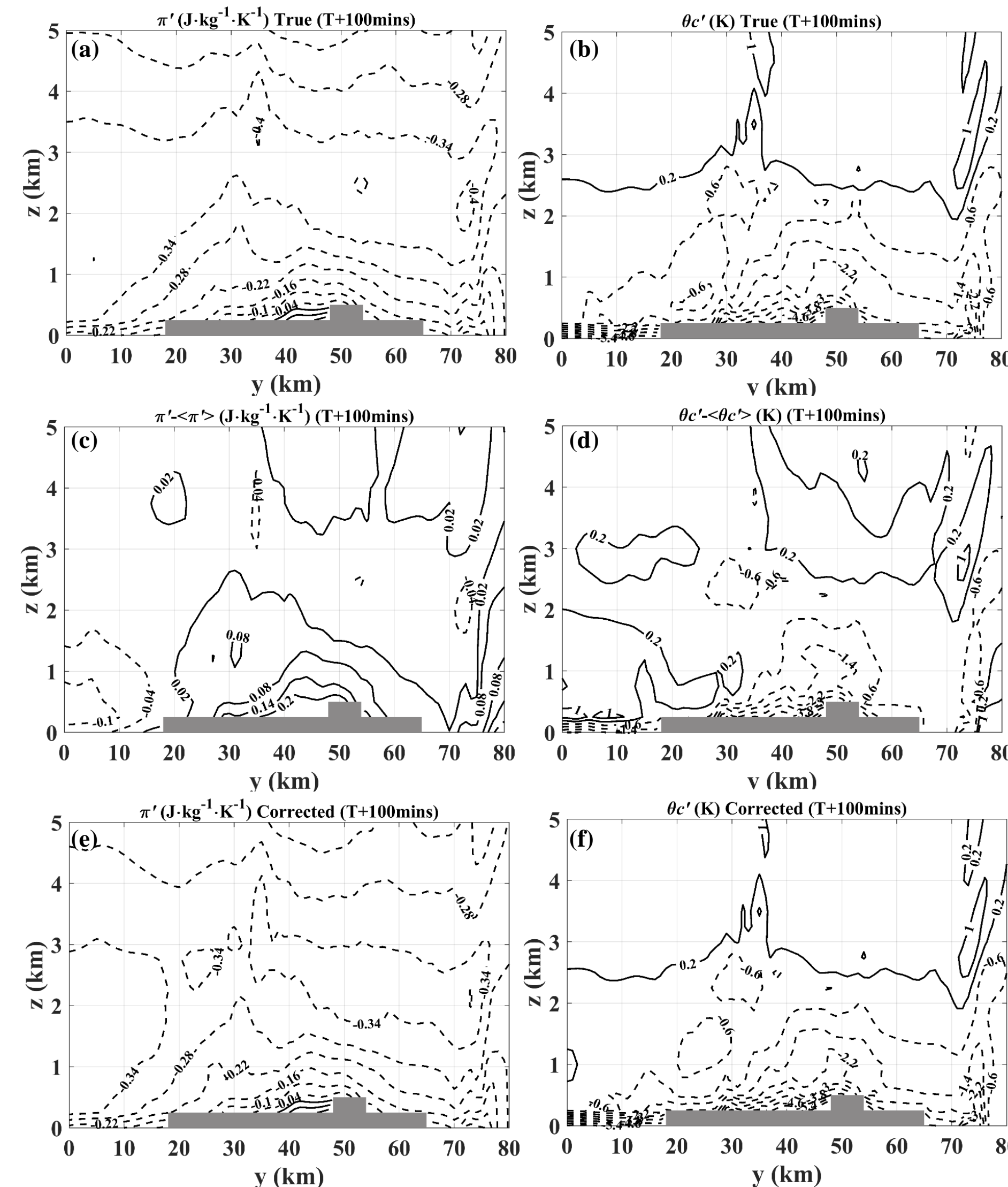


Figure 1 The true (solid line) and retrieved (dashed line): (a) $\langle \pi' \rangle$; and (b) $\langle \theta'_c \rangle$ profiles.

Figure 2 The thermodynamic fields over a vertical cross section: (a) and (b) are the true π' and θ'_c ; (c) and (d) are the deviation of the π' and θ'_c from their horizontal average retrieved by G78 method; (e) and (f) are the retrieved π' and θ'_c after the correction. The grey area denotes terrain.



5. Results from a real test study (2008 SoWMEX field experiment)

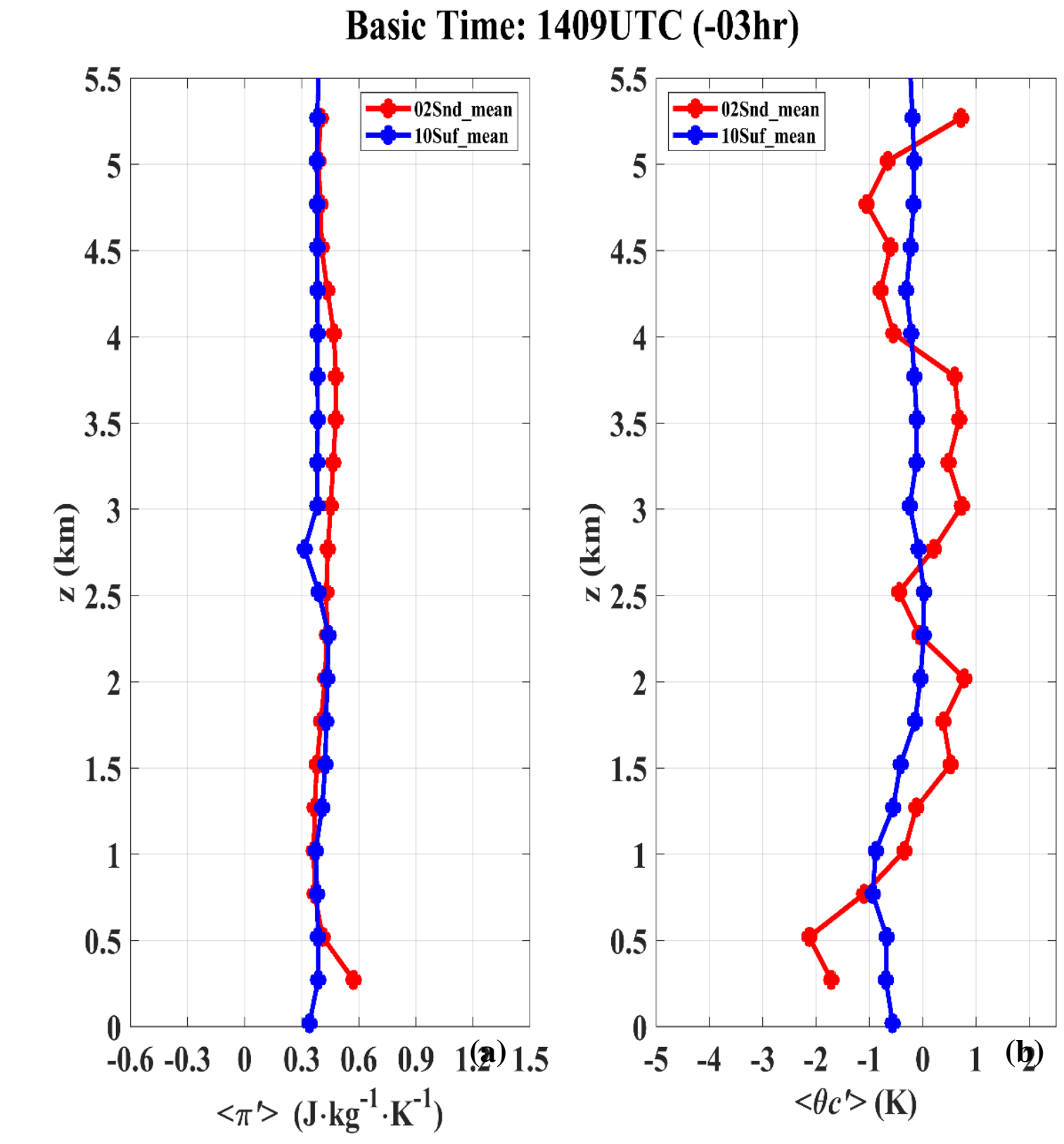


Figure 3 The true and retrieved: (a) $\langle \pi' \rangle$; and (b) $\langle \theta'_c \rangle$ profiles from 2008 SoWMEX IOP8. Red lines are obtained from sounding data, considered as the truth. Blue lines are the retrieved profiles from our new vertical integration method.

6. Summary and future extension

By applying the EoS, the vertical ambiguity that exists in the G78-retrieved thermodynamic variables can be estimated and removed. The only in-situ observations needed to start the vertical integration are the pressure and temperature measured at a single surface station. **This is a new approach for solving an old problem raised since 1987.**

In theory the vertical integrations can also be performed downward. Thus, the vertical integrations may start from a layer located at middle or high altitudes, meaning the in-situ temperature and pressure can be measured at a mountain station (Fig. 4, Fig. 5), or by sensors on board airborne dual-Doppler radars.

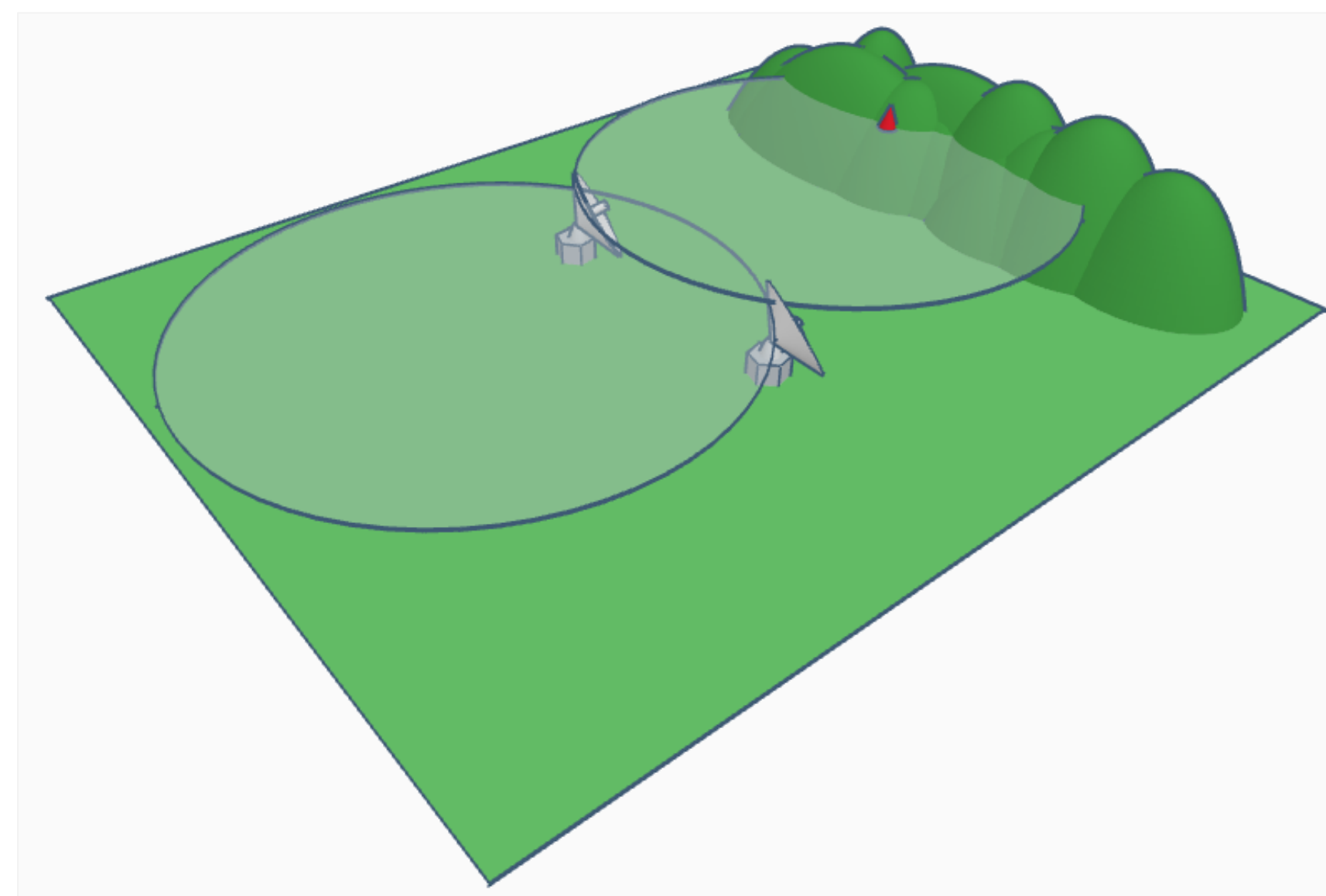


Figure 4 The relative positions of radars, dual-Doppler lobes, terrain, and a mountain station (represented by a red dot) where the in-situ pressure and temperature can be measured.

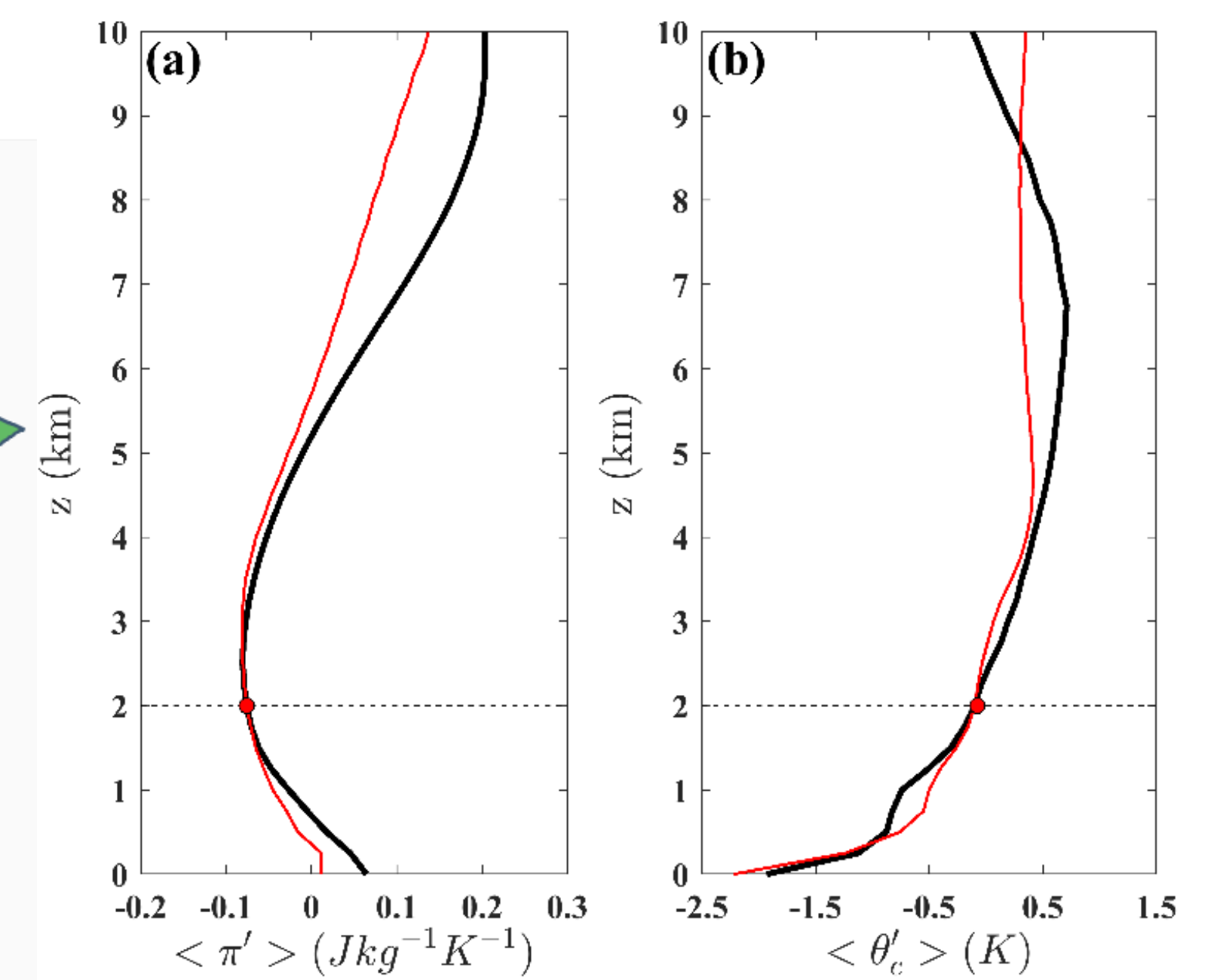


Figure 5 The true (black line) and retrieved (red line) (a) $\langle \pi' \rangle$; (b) $\langle \theta'_c \rangle$ profiles obtained by performing an upward/downward integration from $Z=2.0$ km to the top/bottom of the domain.

Acknowledgment

This research was supported by the National Science and Technology Council of Taiwan under 110-2625-M-008-001, 110-2111-M-008-032, and 111-2111-M-008-020.

References

- Gal-Chen, T., 1978: A method for the initialization of the anelastic equations: Implications for matching models with observations. *Mon. Wea. Rev.*, **106**, 587–606.
- Liou, Y.-C., S.-F. Chang, and J. Sun, 2012: An application of the Immersed Boundary Method for recovering the three-dimensional wind fields over complex terrain using multiple-Doppler radar data. *Mon. Wea. Rev.*, **140**, 1603–1619.
- Liou, Y.-C., P.-C. Yang, and W.-Y. Wang, 2019: Thermodynamic recovery of the pressure and temperature fields over complex terrain using wind fields derived by multiple-Doppler radar synthesis. *Mon. Wea. Rev.*, **147**, 3843–3857.
- Liou, Y.-C. and Y.-L. Teng, 2023: Removal of the vertical structure ambiguity in the thermodynamic retrieval from multiple-Doppler radar synthesized wind fields. *Mon. Wea. Rev.*, **151**, 1427–1442.

